

Chemistry on Rotating Grain Surface: Ro-Thermal Desorption of Molecules from Ice Mantles

THIEM HOANG,^{1,2} NGO-DUY TUNG,³

¹*Korea Astronomy and Space Science Institute, Daejeon 34055, Republic of Korea; thiemhoang@kasi.re.kr*

²*University of Science and Technology, Korea, (UST), 217 Gajeong-ro Yuseong-gu, Daejeon 34113, Republic of Korea*

³*University of Science and Technology of Hanoi, VAST, 18 Hoang Quoc Viet, Hanoi, Vietnam*

ABSTRACT

It is widely believed that water and complex organic molecules (COMs) first form in the ice mantle of dust grains and are subsequently returned into the gas due to grain heating by intense radiation of protostars. Previous research on the desorption of molecules from the ice mantle assumed that grains are at rest which is contrary to the fact that grains are suprathermally rotating as a result of their interaction with an anisotropic radiation or gas flow. To clearly understand how molecules are released in to the gas phase, the effect of grain suprathermal rotation on surface chemistry must be quantified. In this paper, we study the effect of suprathermal rotation of dust grains spun-up by radiative torques on the desorption of molecules from icy grain mantles around protostars. We show that centrifugal potential energy due to grain rotation reduces the potential barrier of molecules and significantly enhances their desorption rate. We term this mechanism *rotational-thermal* or *ro-thermal* desorption. We apply the ro-thermal mechanism for studying the desorption of molecules from icy grains which are simultaneously heated to high temperatures and spun-up to suprathermal rotation by an intense radiation of protostars. We find that ro-thermal desorption is much more efficient than thermal desorption for molecules with high binding energy such as water and COMs. Our results have important implications for understanding the origin of COMs detected in star-forming regions and call for attention to the effect of suprathermal rotation of icy grains to use molecules as a tracer of physical conditions of star-forming regions.

Keywords: dust, extinction, astrochemistry - astrobiology - ISM: molecules

1. INTRODUCTION

To date, more than 200 different molecules, including water and complex organic molecules (COMs, having more than six atoms), were detected in the interstellar medium (see e.g., Caselli & Ceccarelli 2012 for a review). It is thought that COMs form in the ice mantle of dust grains during the warming up phase induced by protostars (see Herbst & van Dishoeck 2009 for a review). However, the question of how such molecules are returned into the gas remains unclear (van Dishoeck 2017).

Several desorption mechanisms have been proposed to explain the desorption of molecules from the icy grain mantle, including thermal and non-thermal mechanisms (see van Dishoeck (2014) for a review). Thermal sublimation (Watson & Salpeter 1972; Leger et al. 1985; Hasegawa et al. 1992) is the most popular mechanism to explain the detection of water and COMs in hot cores/corinos around massive/low-mass protostars because in these regions icy grains can be heated to high temperatures above 100 K (Herbst & van Dishoeck 2009;

Caselli & Ceccarelli 2012). Nevertheless, COMs are frequently detected in lukewarm envelopes around protostars where the temperature is below their sublimation threshold ($T \sim 50 - 100$ K; Oberg et al. 2013; Fayolle et al. 2015; van Dishoeck et al. 2013; Oberg 2016). This casts doubt on the proxy of thermal sublimation. Moreover, non-thermal desorption mechanisms include desorption induced by cosmic rays such as whole grain heating or impulsive heating (CRs; Leger et al. 1985), desorption by single UV photons (photodesorption; Oberg et al. 2009). The UV photodesorption is a promising mechanism to desorb molecules in cold dark clouds in which UV photons can be produced by penetration of CRs. However, these mechanisms are still difficult to quantify for astrophysical conditions, and their resulting products may be clusters rather than individual molecules.

Previous research on thermal and non-thermal desorption of molecules from the grain mantle assumed that grains are at rest, which is contrary to the fact that grains are rapidly rotating due to collisions with

gas atoms and interstellar photons (Draine & Lazarian 1998; Hoang et al. 2010). To accurately understand how molecules are released into the gas, the effect of grain suprathermal rotation on gas-grain chemistry must be quantified. The goal of this paper is to quantify the effect of grain rotation on the desorption of molecules from icy grain mantles.

Interstellar dust grains are known to be rotating suprathermally, as required to reproduce starlight polarization and far-IR/submm polarized dust emission (see Andersson et al. 2015 and Lazarian et al. 2015 for reviews). Purcell (1979) first suggested that dust grains can be spun-up to suprathermal rotation (with velocities larger than grain thermal velocity) by various mechanisms, including the formation of hydrogen molecules on the grain surface. Modern astrophysics establishes that dust grains of irregular shapes can rotate suprathermally due to radiative torques arising from their interaction with an anisotropic radiation field (Draine & Weingartner 1996; Lazarian & Hoang 2007a; Hoang & Lazarian 2008; Hoang & Lazarian 2009; Herranen et al. 2019) or mechanical torques induced by an anisotropic gas flow (Lazarian & Hoang 2007b; Hoang et al. 2018). As a result, in star-forming regions and photodissociation regions (PDRs), strong radiation can both heat dust grains to high temperatures and spin them up to extremely fast rotation, such that resulting centrifugal force would have an important effect on molecule desorption.

Hoang & Tram (2019) first studied the effect of suprathermal rotation induced by radiative torques on the desorption of molecules from the icy grain mantle. For a grain model made of a silicate core covered with a thick ice mantle which is expected in very dense clouds (Oberg et al. 2010), they discovered that the resulting centrifugal force is sufficient to disrupt the entire ice mantle into small fragments. Subsequently, molecules can evaporate from these fragments due to transient heating by UV photons or enhanced thermal sublimation.¹ This process that can desorb the entire ice mantle is then referred to as *rotational desorption*. The rotational desorption mechanism is found to be efficient in an extended region beyond hot cores/corinos surrounding young stellar objects (YSOs). Later on, Tram & Hoang (2019) found that molecules can be directly ejected from ice mantles of suprathermally rotating nanoparticles in CJ-shocks.

¹ In this paper, sublimation and desorption is interchangeably used to imply the desorption of molecules from the grain surface.

Another popular grain model consists of a silicate core, an organic refractory layer and outer ice layer (Greenberg & Li 1996; Greenberg & Li 1997; Jones et al. 2013). For this model, the ice mantle is presumably thin, of tens of monolayers of ice water, such that it is hard to disrupt the entire ice mantle because the resulting tensile stress is insufficient to separate the binding energy between the mantle and the grain core surface as we will show in Section 2. In this case, the joint action of centrifugal force applied to molecules and thermal fluctuations would enhance the rate of thermal sublimation of molecules from the ice mantle, triggering desorption at temperatures below the thermal sublimation threshold. The goal of this paper is to formulate a model of thermal desorption for suprathermally rotating grains and explore its implications for astrochemistry.

The structure of our paper is as follows. In Section 2, we first describe the theory of thermal desorption in the presence of grain rotation, which is termed *rotational-thermal* or *ro-thermal desorption*. In Section 3 we calculate the rate of thermal and ro-thermal desorption for grains spun-up by radiation torques from a strong radiation field. Section 4 discusses the implications of ro-thermal desorption of molecules and polycyclic aromatic hydrocarbons (PAHs) for different astrophysical environments. A summary of our main findings is presented in Section 5.

2. ROTATIONAL-THERMAL DESORPTION OF MOLECULES FROM ICY GRAIN MANTLE

Here we describe our theory for rotational-thermal desorption from rotating grains of angular velocity ω .

2.1. Grain model: Ice mantles on grain surface

Ice mantles are formed on the grain surface due to accretion of gas molecules in cold and dense regions of hydrogen density $n_{\text{H}} = n(\text{H}) + 2n(\text{H}_2) \sim 10^3 - 10^5 \text{ cm}^{-3}$ or the visual extinction $A_V > 3$ (Whittet et al. 1983). Subsequently, more complex molecules, including organic molecules, are thought to form in the ice mantle when grains are being warmed up by intense radiation of protostars (see, e.g., Herbst & van Dishoeck 2009).

Spectral absorption features of H_2O and CO ice are highly polarized (Chrysostomou et al. 1996; Whittet et al. 2008) revealing that icy grain mantles have non-spherical shape and are aligned with magnetic fields (see Lazarian et al. 2015 for a review). Nevertheless, we assume that the grain shape can be described by an equivalent sphere of the same volume with effective radius a .

Figure 1 illustrates a grain model consisting of a silicate core, followed by a refractory carbonaceous mantle, and an outer thin ice mantle. Molecules bind to the ice

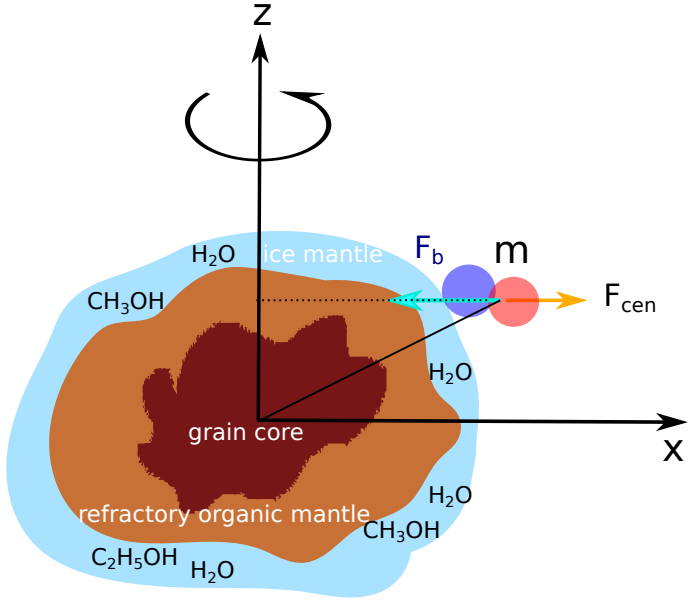


Figure 1. A schematic illustration of a rapidly spinning core-mantle grain of irregular shape. The silicate core is assumed to be compact, which is covered with a refractory organic mantle and the outer, icy water-rich mantle. A molecule of mass m on the ice surface experiences the binding force F_b and centrifugal force F_{cen} which are in opposite directions.

mantle via binding force (F_b) arising from dipole-dipole interaction (van der Waals force) or chemical force. The grain spinning with angular velocity ω induces a centrifugal force (F_{cen}) on the molecule of mass m .

2.2. Thermal desorption rate from non-rotating grains

The problem of thermal desorption from a non-rotating grain is well studied in the literature (Watson & Salpeter 1972; Leger et al. 1985). The underlying physics is that when the grain is heated to high temperatures, molecules on the grain surface acquire kinetic energy from thermal fluctuations within the grain lattice and can escape from the surface.

Let $\tau_{des,0}$ be the desorption rate of molecules with binding energy E_b from a grain at rest ($\omega = 0$) which is heated to temperatures T_d . Following Watson & Salpeter (1972), one has

$$\tau_{sub,0}^{-1} = \nu \exp\left(-\frac{E_b}{kT_d}\right), \quad (1)$$

where ν is the characteristic frequency given by

$$\nu = \left(\frac{2N_s E_b}{\pi^2 m}\right)^{1/2} \quad (2)$$

with N_s being the surface density of binding sites (Tielens & Allamandola 1987). Typically, $N_s \sim 2 \times 10^{15}$ site cm^{-2} .

Potential Energy

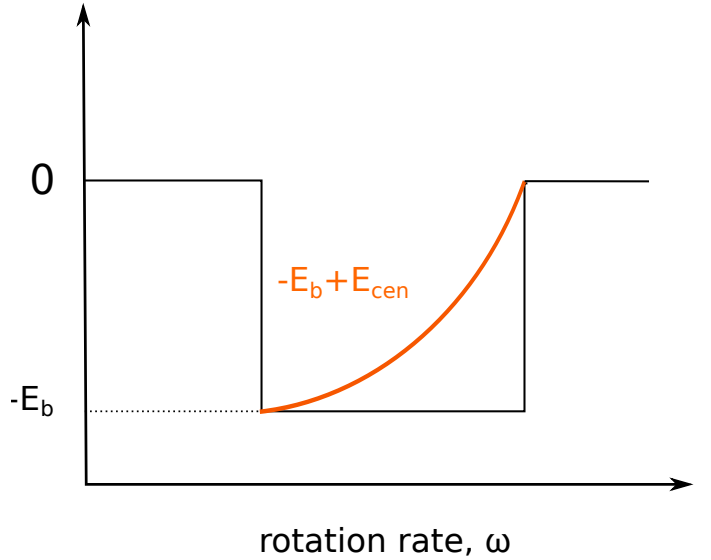


Figure 2. Illustration of the potential energy of a molecule on the rotating grain. The potential barrier is reduced significantly as the angular velocity ω increases as a result of centrifugal potential (E_{cen}).

Table 1. Binding energies and sublimation temperatures for selected molecules on an ice surface

Molecules	E_b/k (K) ^a	T_{sub} (K)
H ₂ O	5700	152 ^b
CH ₃ OH	5530	99 ^b
HCOOH	5570	155 ^c
CH ₃ CHO	2775	30 ^c
C ₂ H ₅ OH	6260	250 ^c
(CH ₂ OH) ₂	10200	350 ^c
NH ₃	5530	78 ^b
CO ₂	2575	72 ^b
H ₂ CO	2050	64 ^b
CH ₄	1300	31 ^b
CO	1150	25 ^b
N ₂	1140	22 ^b

^a See Table 4 in Garrod (2013)

^b See Table 1 from Mumma et al. (1993)

^c See Collings et al. (2004)

Table 1 lists the binding energy and sublimation temperature measured from experiments for popular molecules.

2.3. Ro-thermal desorption rate from rotating grains

In the presence of grain rotation, the centrifugal force acting on a molecule of mass m at distance $r \sin \theta$ from the spinning axis is

$$\mathbf{F}_{\text{cen}} = m\mathbf{a}_{\text{cen}} = m\omega^2 \mathbf{r} \sin \theta = m\omega^2 \sin \theta (x\hat{\mathbf{x}} + y\hat{\mathbf{y}}), \quad (3)$$

where \mathbf{a}_{cen} is the centrifugal acceleration.

We can define centrifugal potential ϕ_{cen} such as $\mathbf{a}_{\text{cen}} = -\nabla\phi_{\text{cen}}$. Then, the corresponding potential is

$$\phi_{\text{cen}} = \omega^2 \sin^2 \theta \left(\frac{x^2 + y^2}{2} \right) = \frac{1}{2} \omega^2 \sin^2 \theta r^2. \quad (4)$$

Assuming that molecules are uniformly distributed over the grain surface, then, one can obtain the average centrifugal potential as follows:

$$\langle \phi_{\text{cen}} \rangle = \frac{\omega^2 a^2 \langle \sin^2 \theta \rangle}{2} = \frac{\omega^2 a^2}{3}, \quad (5)$$

where $\langle \sin^2 \theta \rangle = 2 \int_0^{\pi/2} \sin^2 \theta \sin \theta d\theta = 2/3$.

As a result, the *effective* binding energy of the molecule becomes

$$E_{b,\text{rot}} = E_b - m\langle \phi_{\text{cen}} \rangle, \quad (6)$$

which means that molecules only need to overcome the reduced potential barrier of $E_b - E_{\text{cen}}$ where $E_{\text{cen}} = m\langle \phi_{\text{cen}} \rangle$ to be ejected from the grain surface. The rotation effect is more important for molecules with higher mass and low binding energy.

Figure 2 illustrates the potential barrier of molecules on the surface of a rotating grain as a function of ω . For slow rotation, the potential barrier is determined by binding force. As ω increases, the potential barrier is decreased due to the contribution of centrifugal potential.

The molecule is instantaneously ejected from the surface if the grain is spinning sufficiently fast such that $E_{b,\text{rot}} = 0$. From Equation (6), one can obtain the critical angular velocity for the direct ejection as follows:

$$\omega_{\text{ej}} = \left(\frac{3E_b}{ma^2} \right)^{1/2} \simeq \frac{10^{10}}{a_{-5}} \left(\frac{(E_b/k) m_{\text{CO}}}{1300 \text{ K } m} \right)^{1/2} \text{ rad s}^{-1}, \quad (7)$$

where $a_{-5} = a/(10^{-5} \text{ cm})$.

The ejection angular velocity decreases with increasing grain size and molecule mass m , but it increases with the binding energy E_b .

The rate of ro-thermal desorption (sublimation) rate is given by

$$\tau_{\text{sub,rot}}^{-1} = \nu \exp \left(-\frac{E_b - m\langle \phi_{\text{cen}} \rangle}{kT_d} \right), \quad (8)$$

where the subscript sub stands for sublimation, and the second exponential term describes the probability of desorption induced by centrifugal potential.

Equation (8) can be written as

$$\tau_{\text{sub,rot}}^{-1} = \tau_{\text{sub,0}}^{-1} RD(\omega), \quad (9)$$

where the function $RD(\omega)$ describes the effect of grain rotation on the thermal desorption as given by

$$\begin{aligned} RD(\omega) &= \exp \left(\frac{m\langle \phi_{\text{cen}} \rangle}{kT_d} \right) = \exp \left(\frac{m\omega^2 a^2}{3kT_d} \right) \\ &\simeq 1.7 \exp \left[a_{-5}^2 \left(\frac{m}{m_{\text{CO}}} \right) \left(\frac{\omega}{10^9 \text{ s}^{-1}} \right)^2 \left(\frac{20 \text{ K}}{T_d} \right) \right] \end{aligned} \quad (10)$$

which indicates the rapid increase of ro-thermal desorption rate with the grain size a and angular velocity ω .

Let $\tilde{\omega} = \omega/\omega_T$ be the suprathreshold rotation parameter where $\omega_T = (2kT/I)^{1/2} \simeq 2 \times 10^5 a_{-5}^{-5/2} T_2^{1/2} \text{ rad s}^{-1}$ with T gas temperature and $T_2 = T/100 \text{ K}$, and $I = 8\pi\rho a^5/15$ inertia moment of grains with mass volume density ρ . Then, one obtains

$$RD(\omega) = \exp \left(\frac{2ma^2 T}{3I T_d} \tilde{\omega}^2 \right) = \exp \left(\frac{5m T}{3M T_d} \tilde{\omega}^2 \right) \quad (11)$$

where $M = 4\pi\rho a^3/3$ is the grain mass.

Figure 3 shows the ratio of ro-thermal to thermal sublimation rate, $RD(\omega)$, as a function of the grain angular velocity. For a given grain temperature, the rate of ro-thermal desorption increases exponentially with the angular velocity ω when ω is approaching ω_{ej} (Eq. 7).

2.4. Sublimation temperatures from rotating grains

Let $T_{\text{sub,0}}$ be the sublimation temperature of grains at rest, i.e., $\omega = 0$. The sublimation temperature of rotating grains is denoted by $T_{\text{sub,rot}}$. To quantify the effect of grain rotation on thermal desorption, we compare the grain temperature that is required to produce the same sublimation rate from a non-rotating grain which corresponds to $\tau_{\text{sub,0}}(T_{\text{sub,0}}) = \tau_{\text{sub,rot}}(T_{\text{sub,rot}})$. Thus, one obtains

$$T_{\text{sub,rot}} = \left(1 - \frac{m\langle \phi_{\text{cen}} \rangle}{E_b} \right) T_{\text{sub,0}}. \quad (12)$$

The effect of grain rotation reduces the sublimation temperature as given by

$$\begin{aligned} \frac{T_{\text{sub,0}} - T_{\text{sub,rot}}}{T_{\text{sub,0}}} &= \left(\frac{m\langle \phi_{\text{cen}} \rangle}{E_b} \right) = \left(\frac{ma^2\omega^2}{3E_b} \right) \\ &\simeq 0.14 a_{-5}^2 \left(\frac{\omega}{5 \times 10^9 \text{ s}^{-1}} \right)^2 \left(\frac{m}{m_{\text{CO}}} \right) \left(\frac{2000 \text{ K}}{(E_b/k)} \right). \end{aligned} \quad (13)$$

One can see that the the ro-thermal sublimation temperature can be decreased by 50% for grains of $a = 0.2 \mu\text{m}$ rotating at $\omega = 5 \times 10^9 \text{ rad s}^{-1}$.

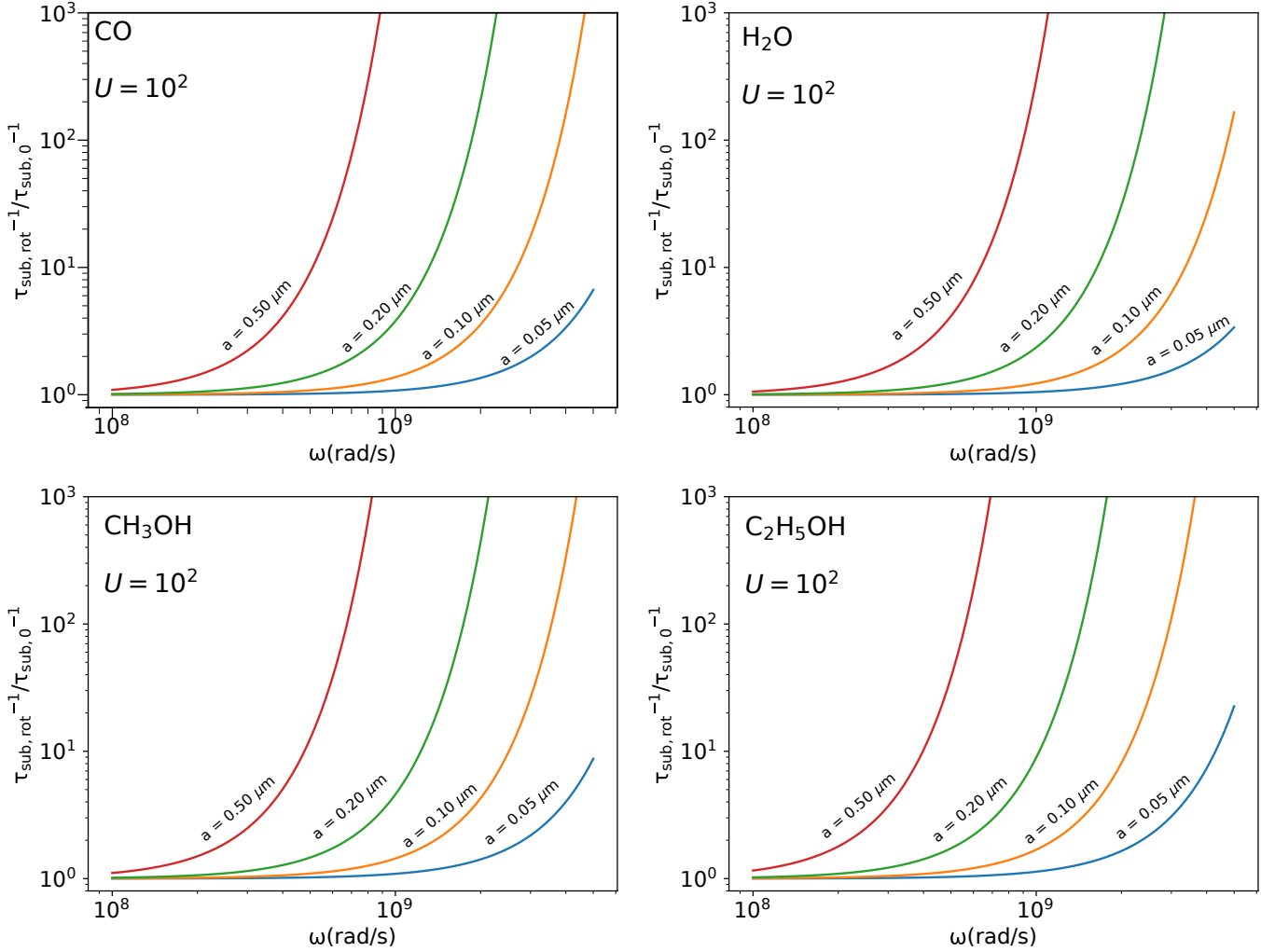


Figure 3. The ratio of ro-thermal desorption rate to thermal desorption rate as a function of grain angular velocity ω computed for the different molecules and different grain sizes, assuming the grain temperature of $T_d \approx 35.5$ K ($U = 100$). The ro-thermal desorption efficiency increases with increasing ω and the grain size a .

3. RO-THERMAL DESORPTION FROM GRAINS SPUN-UP BY RADIATIVE TORQUES

In this section, we will apply the theory formulated in the preceding section for the situation in which grains are rotating suprathermally as a result of the spin-up by Radiative Torques (RATs, e.g., [Draine & Weingartner 1996](#)).

3.1. Centrifugal potential due to radiative torques

Following [Hoang \(2019\)](#), subject to a radiation field of anisotropy degree γ , mean wavelength $\bar{\lambda}$, and radiation strength U , dust grains of size a can be spun-up to a maximum rotation rate by (RATs):

$$\omega_{\text{RAT}} \simeq 9.6 \times 10^8 \gamma a_{-5}^{0.7} \bar{\lambda}_{0.5}^{-1.7} \times \left(\frac{U}{n_1 T_2^{1/2}} \right) \left(\frac{1}{1 + F_{\text{IR}}} \right) \text{ rad s}^{-1}, \quad (14)$$

for grains with $a \lesssim \bar{\lambda}/1.8$, and

$$\omega_{\text{RAT}} \simeq 1.78 \times 10^{10} \gamma a_{-5}^{-2} \bar{\lambda}_{0.5} \times \left(\frac{U}{n_1 T_2^{1/2}} \right) \left(\frac{1}{1 + F_{\text{IR}}} \right) \text{ rad s}^{-1}, \quad (15)$$

for grains with $a > \bar{\lambda}/1.8$. Here, $n_1 = n_{\text{H}}/(10 \text{ cm}^{-3})$, $\bar{\lambda}_{0.5} = \bar{\lambda}/(0.5 \mu\text{m})$, F_{IR} is the dimensionless parameter describing the grain rotational damping by infrared emission that depends on $(n_{\text{H}}, T_{\text{gas}}, U)$ ([Draine & Lazarian 1998](#); [Hoang et al. 2010](#)), and $U = u_{\text{rad}}/u_{\text{ISRF}}$ with u_{rad} the total radiation energy density and u_{ISRF} the energy density of the standard interstellar radiation field (ISRF) in the solar neighborhood ([Mathis et al. 1983](#); [Hoang et al. 2019](#)). The rotation rate depends on the parameter $U/n_{\text{H}} T_{\text{gas}}^{1/2}$ and the damping by far-infrared emission F_{IR} .

For convenience, let $a_{\text{trans}} = \bar{\lambda}/1.8$ which denotes the grain size at which the RAT efficiency changes between the power law and flat stages (see e.g., Lazarian & Hoang 2007a; Hoang et al. 2019), and ω_{RAT} changes from Equation (14) to (15).

Plugging ω_{RAT} into Equation (5), one obtains the centrifugal potential due to grain rotation as follows:

$$m\langle\phi_{\text{cen}}\rangle = 1.8 \times 10^{-3} \gamma^2 a_{-5}^{3.4} \bar{\lambda}_{0.5}^{-3.4} \left(\frac{m}{m_{\text{CO}}} \right) \times \left(\frac{U}{n_1 T_2^{1/2}} \right)^2 \left(\frac{1}{1 + F_{\text{IR}}} \right)^2 \text{ eV} \quad (16)$$

for $a \lesssim a_{\text{trans}}$ and

$$m\langle\phi_{\text{cen}}\rangle = 0.6 \gamma^2 a_{-5}^{-2} \bar{\lambda}_{0.5}^2 \left(\frac{m}{m_{\text{CO}}} \right) \times \left(\frac{U}{n_1 T_2^{1/2}} \right)^2 \left(\frac{1}{1 + F_{\text{IR}}} \right)^2 \text{ eV} \quad (17)$$

for $a > a_{\text{trans}}$.

The centrifugal potential increases rapidly with the grain size as $a^{3.4}$ until $a = a_{\text{trans}}$ (Eq. 16), and it increases with the radiation strength as U^2 . Thus, this potential is important for strong radiation fields.

Using the centrifugal potentials (Eqs. 16 and 17) one can calculate the rate of ro-thermal desorption (Eq. 8) and the temperature threshold for ro-thermal desorption (Eq. 12).

3.2. Radiation strength required for rotational desorption of molecules

In addition to the ro-thermal desorption, individual molecules can be directly ejected by centrifugal forces when the rotational rate is sufficiently high. This process is termed *rotational desorption* in Tram & Hoang (2019). Comparing ω_{RAT} with ω_{ej} (Eq. 7), one can then derive the critical radiation strength at which the molecule is immediately ejected

$$U_{\text{ej}} \simeq 8 n_1 T_2^{1/2} (1 + F_{\text{IR}}) \frac{\lambda_{0.5}^{1.7}}{\gamma a_{-5}^{1.7}} \left(\frac{(E_b/k) m_{\text{CO}}}{1300 \text{ K } m} \right)^{1/2} \quad (18)$$

for $a \lesssim a_{\text{trans}}$, and

$$U_{\text{ej}} \simeq 0.4 n_1 T_2^{1/2} (1 + F_{\text{IR}}) \frac{\lambda_{0.5}^{1.7} a_{-5}}{\gamma} \left(\frac{(E_b/k) m_{\text{CO}}}{1300 \text{ K } m} \right)^{1/2} \quad (19)$$

for $a > a_{\text{trans}}$.

3.3. Radiation strength required for rotational desorption of entire ice mantles

As shown in Hoang & Tram (2019), when the rotation rate is sufficiently high such as the tensile stress acting on the interface between a thick ice mantle and the grain core exceeds the maximum limit of the ice mantle, $S_{\text{max}} \sim 10^7 \text{ erg cm}^{-3}$, the ice mantle is disrupted into smaller fragments. In the case of a thin ice mantle, the tensile strength is replaced by the adhesive strength, which depends on the mechanical property of the surface and grain temperature. The adhesive strength is low for clean surface, but it can reach $\sim 10^9 \text{ erg cm}^{-3}$ for rough surfaces (Work & Lian 2018).

Let l_m be the ice mantle thickness and x_0 be the distance from the core-mantle interface to the spinning axis. From Equation (7) in Hoang & Tram (2019), one obtains the tensile stress on the ice mantle:

$$S_x \simeq 2.5 \times 10^9 \hat{\rho}_{\text{ice}} \omega_{10}^2 a_{-5}^2 \left[1 - \left(\frac{x_0}{a} \right)^2 \right] \text{ erg cm}^{-3} \quad (20)$$

where $\hat{\rho}_{\text{ice}} = \rho_{\text{ice}}/(1 \text{ g cm}^{-3})$ and $\omega_{10} = \omega/(10^{10} \text{ rad s}^{-1})$. For a thin mantle layer of $l_m = a - x_0 \ll a$, one has

$$S_x \simeq 5 \times 10^8 \hat{\rho}_{\text{ice}} \omega_{10}^2 a_{-5} l_{-6} \text{ erg cm}^{-3}, \quad (21)$$

where $x_0 + a \approx 2a$ is assumed, and $l_{-6} = l_m/(10^{-6} \text{ cm})$. The critical rotational velocity is determined by $S_x = S_{\text{max}}$:

$$\omega_{\text{disr}} = \frac{2}{a(1 - x_0^2/a^2)^{1/2}} \left(\frac{S_{\text{max}}}{\rho_{\text{ice}}} \right)^{1/2} \simeq \frac{4.5 \times 10^{10}}{a_{-5}^{1/2} l_{-6}^{1/2}} \hat{\rho}_{\text{ice}}^{-1/2} S_{\text{max},9}^{1/2} \text{ rad s}^{-1}, \quad (22)$$

where $S_{\text{max},9} = S_{\text{max}}/(10^9 \text{ erg cm}^{-3})$.

The critical radiation strength to disrupt the ice mantle is then

$$U_{\text{disr}} \simeq 32.5 n_1 T_2^{1/2} \frac{(1 + F_{\text{IR}})}{l_{-6}^{1/2}} \left(\frac{\lambda_{0.5}^{1.7}}{\gamma a_{-5}^{1.2}} \right) S_{\text{max},9}^{1/2} \quad (23)$$

for $a \lesssim a_{\text{trans}}$, and

$$U_{\text{disr}} \simeq 1.8 n_1 T_2^{1/2} \frac{(1 + F_{\text{IR}})}{l_{-6}^{1/2}} \left(\frac{\lambda_{0.5}^{1.7} a_{-5}^{1.5}}{\gamma} \right) S_{\text{max},9}^{1/2} \quad (24)$$

for $a > a_{\text{trans}}$.

For grains with a compact core, the tensile strength $S_{\text{max}} \sim 10^9 \text{ erg cm}^{-3}$ is expected (see e.g., Hoang et al. 2019). Comparing ω_{ej} from Equation (18) with ω_{disr} from Equation (23), one can see that ro-thermal desorption of individual molecules can occur before the disruption of ice mantle if the ice mantle thickness is below 100 monolayers of water ice (i.e., $l_m < 200 \text{ \AA}$).

3.4. Radiation strength required for thermal desorption

Under strong radiation fields, icy grains are heated to an equilibrium temperature, which can be approximately given by $T_d \simeq 16.4a_{-5}^{-1/15}U^{1/6}$ K for silicate-core grains (Draine 2011). One can then derive the radiation strength required for the classical thermal sublimation at $T_d = T_{\text{sub},0}$:

$$U_{\text{sub}} \simeq 6 \times 10^{11} a_{-5}^{6/15} \left(\frac{T_{\text{sub},0}}{1500 \text{ K}} \right)^6. \quad (25)$$

Comparing U_{sub} with U_{ej} , U_{disr} one can see that the required radiation strength for thermal desorption is many orders of magnitude higher than ro-thermal desorption as well as direct ejection. One note that, for the same radiation strength U , graphite grains can be heated to temperatures higher than silicates by $\sim 30\%$, but their sublimation threshold is more than two times higher than silicates. As a result, the value of U_{sub} for graphite grains is much larger.

3.5. Numerical results

3.5.1. Rates of ro-thermal vs. thermal desorption

To calculate the rate of ro-thermal desorption, we first compute the rotation rate spun-up by RATs as given by Equations (14) and (15). Here we adopt $\gamma = 0.7$ for the anisotropy degree of the radiation field as in Draine & Weingartner (1996) for molecular clouds (see also Bethell et al. 2007).² We then calculate the ro-thermal desorption rate of different molecules from the surface of spinning dust grains. We consider the different gas density and radiation strengths and assume thermal equilibrium between gas and dust, i.e., $T = T_d$ which is valid for dense regions around protostars. Our calculations are performed for several popular molecules, including methanol, ethanol, with binding energy listed in Table 1.

Figure 4 shows the rate of thermal desorption (without rotation) and ro-thermal desorption (with rotation) as a function of the radiation strength U assuming a typical grain size $a = 0.2 \mu\text{m}$ and stellar radiation spectrum with $\bar{\lambda} = 0.5 \mu\text{m}$. The corresponding grain temperatures are shown on the top horizontal axis. The ro-thermal desorption rate increases exponentially with the radiation intensity even at temperatures much below the sublimation threshold. In all realizations, the ro-thermal desorption is much faster than thermal desorption except for CO_2 with high density $n_{\text{H}} = 10^5 \text{ cm}^{-3}$. The efficiency of ro-thermal desorption is stronger for lower

gas density n_{H} . This originates from the fact that grains can spin faster due to lower rotational damping by gas collisions. One can also see that for most molecules the ro-thermal desorption occurs well before the immediate ejection threshold marked by U_{ej} .

Figure 5 shows the rate of ro-thermal vs. thermal desorption for $a = 0.1 \mu\text{m}$. Ro-thermal desorption is still faster than thermal desorption, although the efficiency is lower than that for $a = 0.2 \mu\text{m}$ due to lower rotation rate by RATs ω_{RAT} (see Eq. 14).

Figure 6 shows results for N_2 and NH_3 molecules, assuming $a = 0.1 \mu\text{m}$ and $0.2 \mu\text{m}$. The similar trend as other molecules (Figure 4) is observed. The efficiency of ro-thermal desorption is clearly seen for NH_3 which has high sublimation temperature.

Same as Figure 4, but Figure 7 shows the results for attenuated radiation fields with $\bar{\lambda} = 1.2 \mu\text{m}$. The efficiency of ro-thermal desorption is weaker than the case of $\bar{\lambda} = 0.5 \mu\text{m}$, but still dominates over thermal desorption.

Figure 8 shows similar results as Figure 7 but for $\bar{\lambda} = 1.2 \mu\text{m}$. The results are slightly different due to the radiation field with longer mean wavelength $\bar{\lambda}$.

3.5.2. Temperature threshold for ro-thermal vs. thermal desorption

Figure 9 shows the decrease of sublimation temperature, $\Delta T = |T_{\text{sub,rot}} - T_{\text{sub},0}|$ due to centrifugal potential as a function of the radiation intensity (U) and the grain temperature, assuming the different gas density. Analytical results from Equation (13) are also shown for comparison. The effect of ro-thermal desorption is more important for lower density. Ro-thermal desorption is also more efficient for molecules with higher binding energy where ro-thermal desorption can occur at more than 100 K lower than the thermal desorption. The efficiency of ro-thermal desorption is more efficient for stellar photons of $\bar{\lambda} = 0.5 \mu\text{m}$ but less efficient for reddened photons with $\bar{\lambda} = 1.2 \mu\text{m}$.

At high densities of $n_{\text{H}} = 10^5 \text{ cm}^{-3}$, ro-thermal desorption can still occur at temperatures much lower than thermal desorption for water and other molecules with high binding energy.

Note that the molecule CO_2 has low $E_b \sim 2575 \text{ K}$ but its sublimation temperature is high of $T_{\text{sub},0} \sim 72 \text{ K}$ (Collings et al. 2004), which results in a slightly peaky feature ΔT in Figure 9.

4. DISCUSSION

4.1. Thermal desorption, rotational desorption, ro-thermal desorption

Thermal desorption (sublimation) is a popular mechanism to release water and complex organic molecules

² The anisotropy degree of the diffuse ISRF is lower of $\gamma = 0.1$, and $\gamma = 1$ for unidirectional radiation fields from a point source.

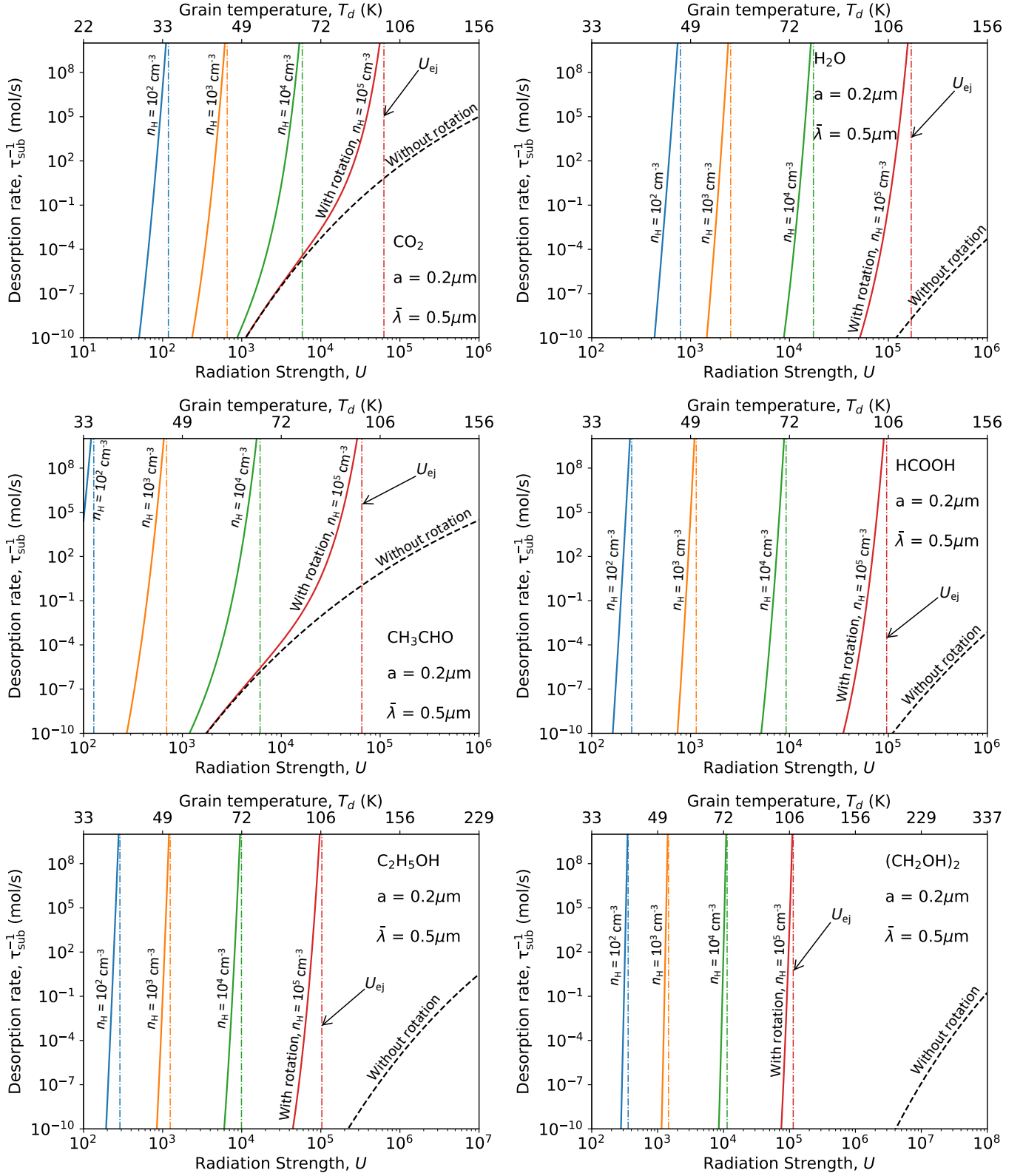


Figure 4. Rates of ro-thermal desorption (solid lines, with rotation) and thermal desorption (dashed line, without rotation) for several molecules as function of the radiation strength (U) and grain temperature (top horizontal axis), assuming grains of size $a = 0.2 \mu\text{m}$ and the mean wavelength $\bar{\lambda} = 0.5 \mu\text{m}$. A range of gas density $n_{\text{H}} = 10^2 - 10^5 \text{ cm}^{-3}$ is considered. The vertical lines show the direct ejection threshold U_{ej} .

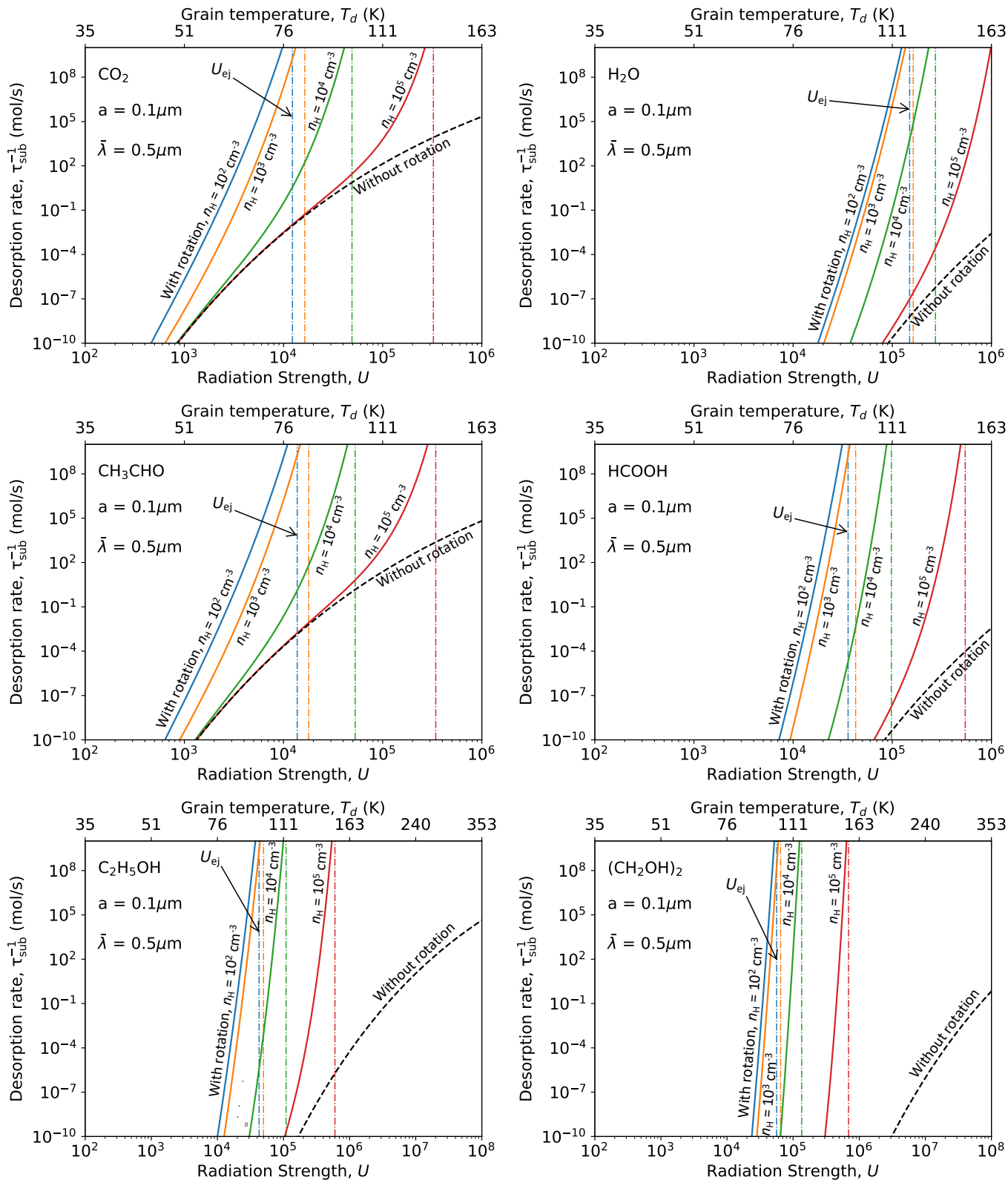


Figure 5. Same as Figure 4 but for grains of size of $a = 0.1 \mu\text{m}$. Due to smaller grain size, the efficiency of ro-thermal desorption is decreased but still dominates over thermal desorption (dashed line).

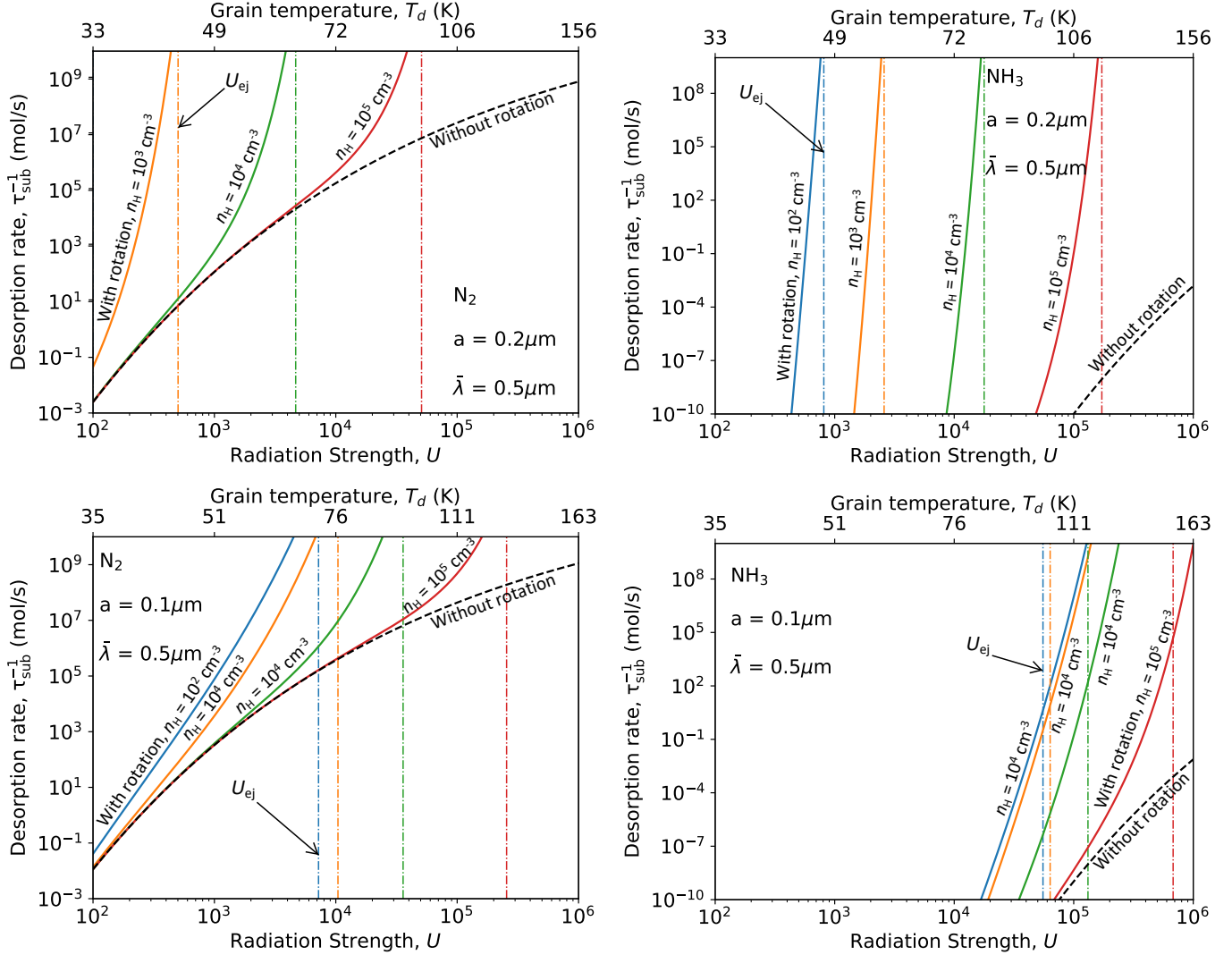


Figure 6. Same as Figure 4 but for N_2 and NH_3 molecules, assuming $a = 0.2 \mu m$ (upper panels) and $a = 0.1 \mu m$ (lower panel). Ro-thermal desorption is much faster than thermal desorption for both molecules.

from the icy grain mantle in star-forming regions (Herbst & van Dishoeck 2009). This desorption process ignores the fact that grains are rapidly spinning due to radiative torques when grains are subject to intense radiation field from protostars (Draine & Weingartner 1996; Hoang & Lazarian 2008; Hoang & Lazarian 2009; Herranen et al. 2019).

The effect of suprathermal rotation on the desorption of molecules from the grain surface is first studied in Hoang & Tram (2019) where the authors discovered that the resulting centrifugal force is sufficient to disrupt the ice mantle into small fragments. Subsequently, molecules can evaporate from these fragments due to transient heating by UV photons or enhanced thermal sublimation. This *rotational* desorption mechanism is found to be efficient in hot cores/corinos around young stars where the radiation strength U can reach

$U \sim 10^8 - 10^9$ (e.g., grain temperature $T \sim 500$ K). The efficiency of rotational desorption increases with the thickness of the ice mantle, so it is most efficient for grains with a thick ice mantle.

In this paper, we study the additional effect of grain rotation on thermal desorption in regions where grain temperatures are below the sublimation threshold of water and molecules, which have $U < 10^6$ or $T < 200$ K. Specifically grain rotation provides molecules on the grain surface with a centrifugal force that acts in the opposite direction from the binding force. As a result, a rather weak level of thermal excitation can help molecules to sublime if grains are spinning rapidly. We term this mechanism *ro-thermal desorption* mechanism. The difference between ro-thermal desorption and rotational desorption is that in the former process molecules sublime directly from the intact icy grain

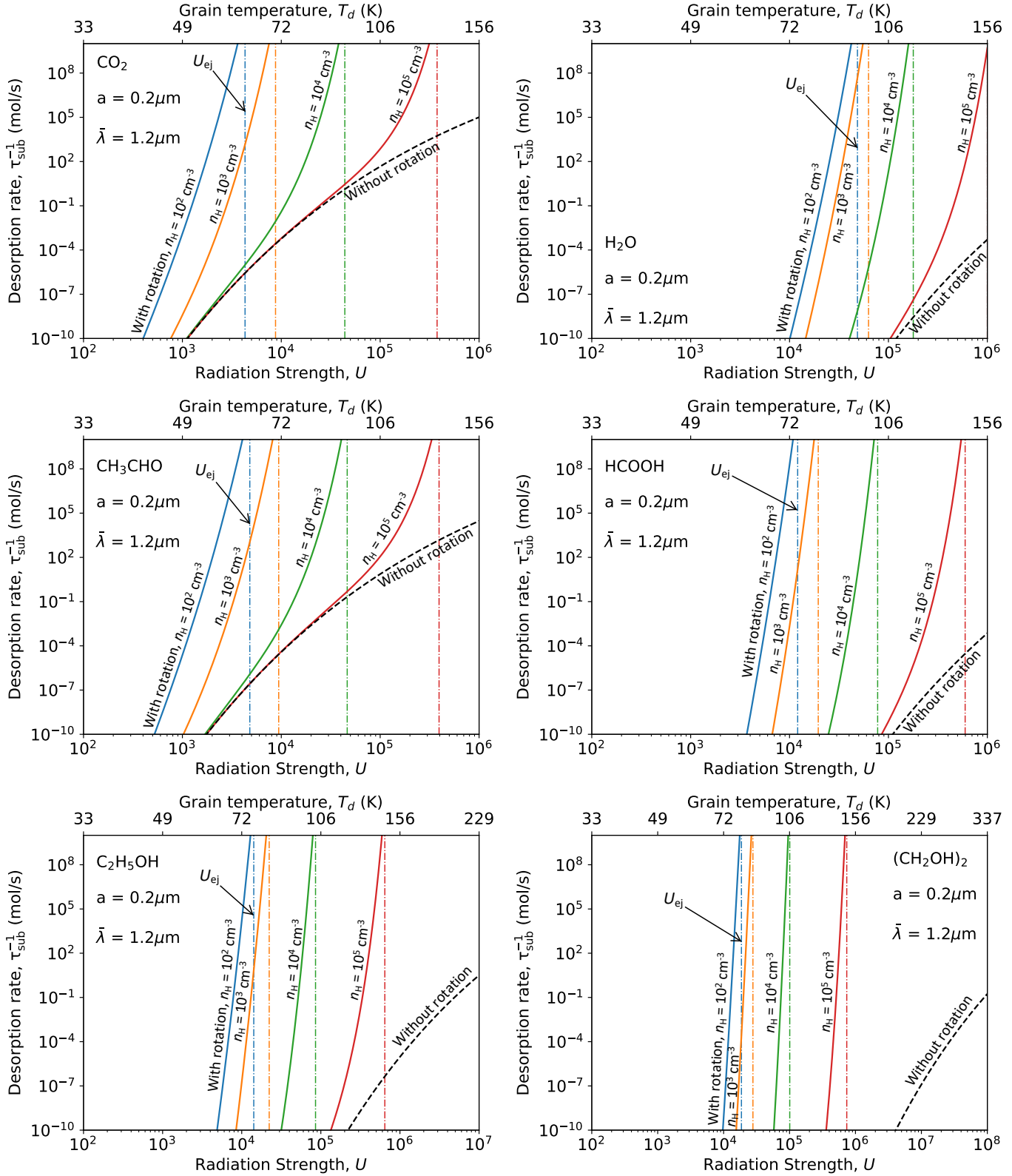


Figure 7. Same as Figure 4 but for the mean wavelength $\bar{\lambda} = 1.2 \mu\text{m}$. Ro-thermal desorption appears to be much faster than thermal desorption.

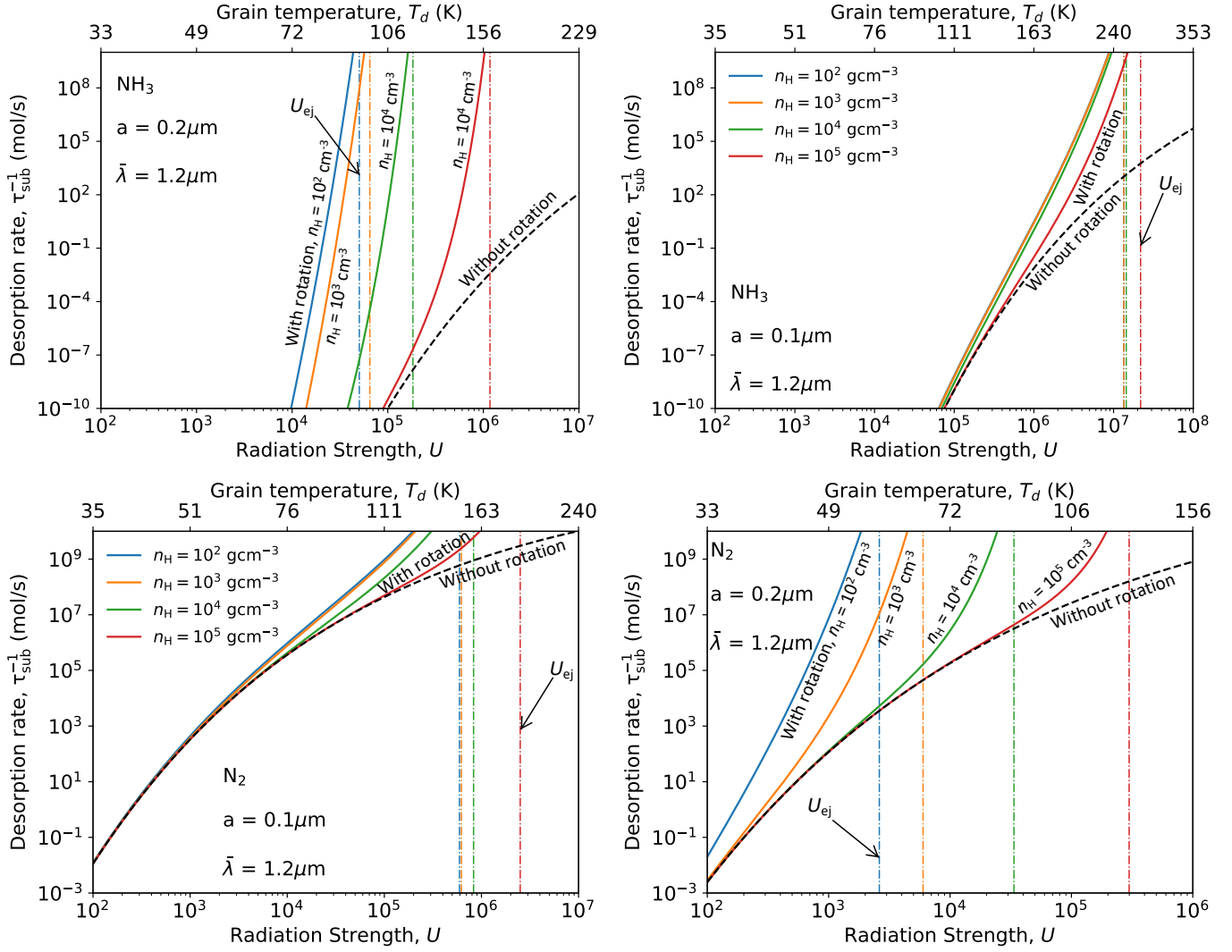


Figure 8. Same as Figure 7 but for N_2 and NH_3 molecules. Ro-thermal desorption is much faster than thermal desorption for both molecules.

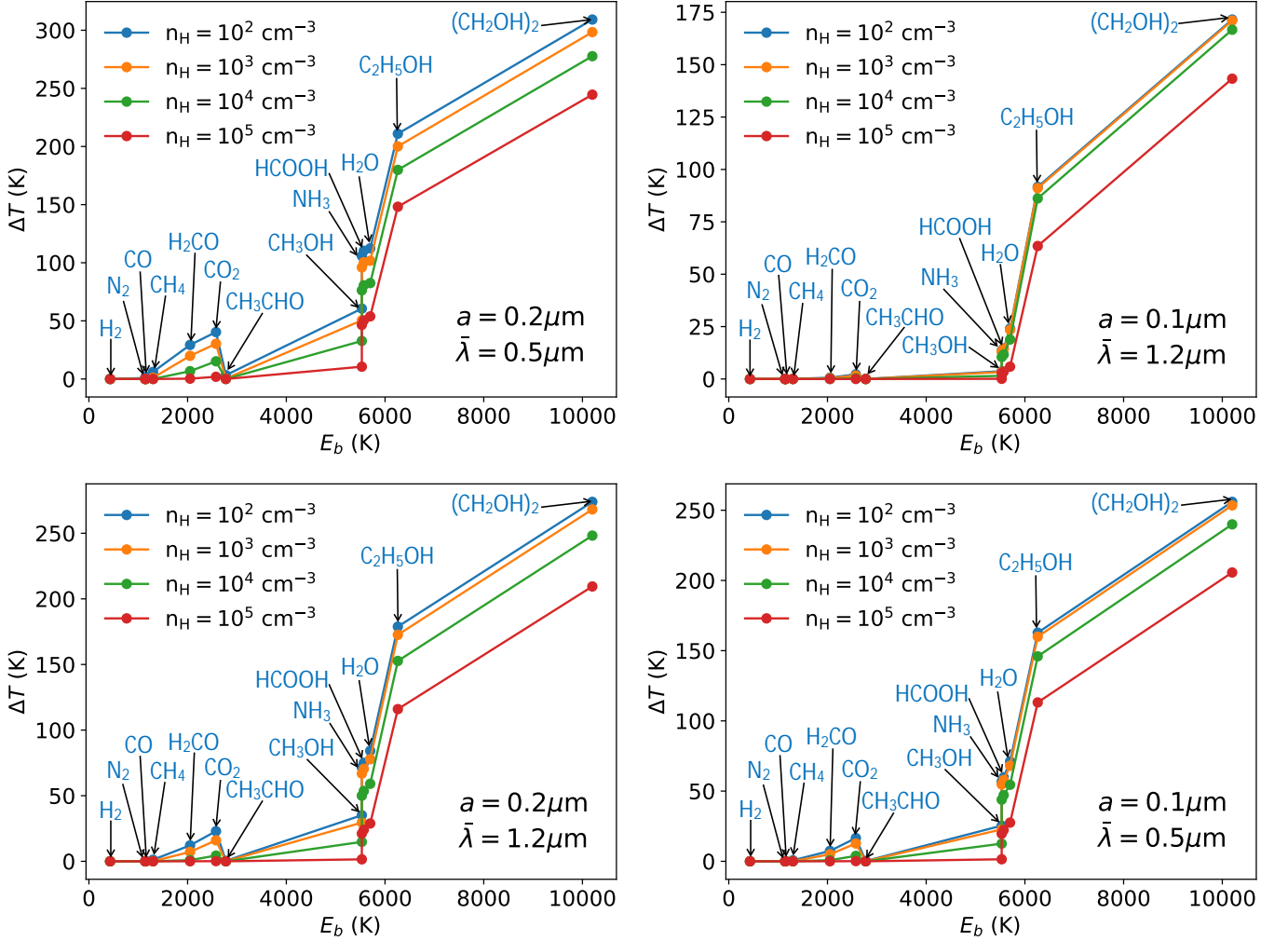


Figure 9. Difference between the temperature of ro-thermal desorption and that of thermal sublimation, $\Delta T = |T_{\text{sub,rot}} - T_{\text{sub},0}|$, as a function of molecule binding energy for $a = 0.1 \mu\text{m}$ and $a = 0.2 \mu\text{m}$ for $\bar{\lambda} = 0.5 \mu\text{m}$ and $1.2 \mu\text{m}$. The difference increases with increasing E_b and with the gas density.

mantle, whereas in the latter process, the ice mantle is first disrupted into tiny icy fragments and subsequently molecules sublimate from these icy fragments.

The efficiency of the ro-thermal desorption depends both on the grain rotation rate and grain temperature, but the rotation rate plays a key role. Therefore, ro-thermal desorption can occur in weak radiation fields when grains can be spun-up by mechanical torques (Lazarian & Hoang 2007b; Hoang et al. 2018). The ro-thermal desorption mechanism takes over rotational desorption when the ice mantle is thin (i.e., $\Delta a_m \ll a$) such that the tensile stress acting on the ice mantle is rather small and cannot desorb the entire mantle (see Figures 4-5).

We also find that individual molecules can be directly ejected from the icy grain mantle for $\omega \gtrsim \omega_{\text{ej}}$, and this rotational desorption process requires higher radiation

strength than ro-thermal desorption (see Figures 4 and 5). Compared to rotational desorption, we find that ro-thermal desorption occurs at lower radiation strength before the entire mantle can be disrupted into small fragments and efficient for thin ice mantle of thickness $l < 100 \text{\AA}$.

Compared to UV photodesorption that requires FUV photons between 7 – 10.5 eV to be effective (Oberg et al. 2007; van Dishoeck et al. 2013), ro-thermal desorption can work with optical photons with the mean wavelength even at $\bar{\lambda} \gtrsim 0.5 \mu\text{m}$. Therefore, ro-thermal desorption can be effective in regions without FUV.

Finally, the rot-thermal desorption mechanism is expected to be most efficient in astrophysical environments with $U/n_{\text{H}}T_{\text{gas}}^{1/2} > 1$ (see Eqs. 14 and 15), such as star-forming regions, the surface and intermediate layer

of protoplanetary disks, reflection nebula (e.g., Hoang et al. 2015), and photodissociation regions.

4.2. Ro-thermal desorption of PAHs

Like other molecules, PAHs condense in the ice mantle of dust grains in cold dense clouds (Bernstein et al. 1999; Cuytle et al. 2014; Cook et al. 2015). Yet, the question of how PAHs are returned into the gas phase is still unclear.

Ro-thermal desorption appears to be an efficient mechanism to desorb PAHs. Since ro-thermal desorption requires lower radiation strength to desorb than rotational desorption, one can describe the efficiency of ro-thermal desorption by considering the ejection threshold. Using Equation (7), one obtains the ejection threshold of PAHs:

$$\omega_{\text{ej}} = \left(\frac{3E_b}{ma^2} \right)^{1/2} \simeq \frac{10^{10}}{a_{-5}} \left(\frac{(E_b/k) m_{\text{C}_6\text{H}_6}}{4000 \text{ K } m} \right)^{1/2} \text{ rad s}^{-1}, \quad (26)$$

where the binding energy of benzene C_6H_6 and naphthalene (C_{10}H_8) to ice is $E_b/k \sim 4000 \text{ K}$ and 6000 K (see Table 4 and 5 in Michoulier et al. 2018).

The ejection radiation strength is then

$$U_{\text{ej}} \simeq 35n_1 T_2^{1/2} (1 + F_{\text{IR}}) \frac{\lambda_{0.5}^{1.7}}{\gamma a_{-5}^{1.7}} \left(\frac{(E_b/k) m_{\text{C}_6\text{H}_6}}{4000 \text{ K } m} \right)^{1/2} \quad (27)$$

for $a \lesssim a_{\text{trans}}$, and

$$U_{\text{ej}} \simeq 1.8n_1 T_2^{1/2} (1 + F_{\text{IR}}) \frac{\lambda_{0.5}^{1.7} a_{-5}}{\gamma} \left(\frac{(E_b/k) m_{\text{C}_6\text{H}_6}}{4000 \text{ K } m} \right)^{1/2} \quad (28)$$

for $a > a_{\text{trans}}$. Clearly, the ejection threshold is much lower than that of water and COMs (see Figures 4-7). Therefore, the ro-thermal desorption is efficient for desorption of PAHs in star-forming regions.

4.3. Ro-thermal desorption in photodissociation regions and protoplanetary disks

Photodissociation regions (PDRs) are traditionally dense molecular clouds with typical gas density $n_{\text{H}} \lesssim 10^5 \text{ cm}^{-3}$ illuminated by O or B stars (e.g., Orion Bar) with radiation strength $U \lesssim 10^5 - 10^6$ (see Hollenbach & Tielens 1999; Tielens, A G G M 2007).

For a typical PDR model like Orion Bar (Allers et al. 2005), the gas density and radiation fields are $n \sim 10^4 \text{ cm}^{-3}$ and $U \sim 3 \times 10^4$. For these physical conditions, from Figures 4 and 5, we see that ro-thermal desorption is very efficient in desorbing water and complex organic molecules. This mechanism can explain the formation of COMs and PAHs which are usually observed in PDRs (see Cuppen et al. 2017 for a review).

The surface and intermediate layer of protoplanetary disks around young stars are attractive targets for studying ro-thermal desorption due to strong radiation fields. For the same radiation intensity, the rate of ro-thermal desorption is several orders of magnitude higher than that of thermal desorption (Spaans et al. 1995).

We note that in more intense radiation field of hot cores/corinos, the entire ice mantle could be desorbed via *rotational desorption* mechanism (Hoang & Tram 2019). Finally, with this paper, the effect of grain rotation on thermal desorption of molecules is complete and for the first time demonstrate the importance of accounting for grain dynamics for grain-surface chemistry.

We note that grains can also be spun-up by mechanical torques (Lazarian & Hoang 2007b; Hoang et al. 2018). Therefore, ro-thermal desorption can occur for supersonic flows. The potential environments include icy grains in young stellar outflows (see Hoang & Tram 2019).

4.4. From experimental data to astrochemical modeling

Astrochemical modeling of observational data usually takes desorption rates and chemical reaction rates measured from experiment and apply directly to interstellar dust grains (e.g., Öberg et al. 2009). Usually, the physical properties of dust grains, including grain surface, grain size, and grain dynamics, are disregarded (see Caselli & Ceccarelli 2012). Recently, the effect of grain surface properties was studied by experiments in Potapov et al. (2019), but the application to the specific grain surface is not yet available.

In light of our findings, application of experimental measurements of sublimation temperatures cannot be directly applied to model thermal sublimation of molecules from the grain mantle due to the effect of grain suprathreshold rotation. We find that the effective sublimation temperature is much lower than the measured temperature for non-rotating grains in the lab, which depends on the local gas density. The difference is significant for water ice and COMs with high binding energy.

5. SUMMARY

We have studied the effect of grain suprathreshold rotation on the thermal desorption of molecules from icy grain mantles. Our results are summarized as follows:

- 1 We find that the centrifugal potential energy due to grain rotation acts to reduce the potential barrier of the molecule desorption and formulate a theory for thermal desorption of molecules from rapidly spinning grains. To differentiate from the classical thermal desorption mechanism, we term

- this mechanism rotational-thermal desorption or ro-thermal desorption.
- 2 We apply the ro-thermal desorption theory for icy grains spun-up by radiative torques and find that the rate of ro-thermal desorption of water and COMs is much larger than that of the classical thermal sublimation.
 - 3 We derive the effective temperature threshold for ro-thermal desorption and find that this temperature is much lower than that for thermal desorption. The ro-thermal desorption temperatures decrease with increasing the radiation strength and with decreasing the gas density.
 - 4 We find that COMs can be released via ro-thermal desorption in environments with low temperatures ($T < 100$ K) provided that the gas density is not very high, i.e., $n_{\text{H}} < 10^8 \text{ cm}^{-3}$. As a result, interpretation of the detection of COMs in astrophysical conditions by means of grain heating only is likely inadequate because of centrifugal force effect.

- 5 To use molecules as a reliable tracer of physical and chemical properties of astrophysical environments, one needs to take into account the effect of suprathreshold rotation of icy grains on desorption of molecules, and chemical modeling should take into account this effect.
- 6 Our results reveal that using experimental data for astrochemical modeling of gas-grain surface chemistry in star-forming regions would be cautious and must account for the effect of suprathreshold rotation of icy grains.

ACKNOWLEDGMENTS

We are grateful to the anonymous referees for helpful comments that improved the presentation of the manuscript. We thank Le Ngoc Tram for useful comments. This work was supported by the National Research Foundation of Korea (NRF) grants funded by the Korea government (MSIT) (2017R1D1A1B03035359 and 2019R1A2C1087045).

REFERENCES

- Allers, K. N., Jaffe, D. T., Lacy, J. H., Draine, B. T., & Richter, M. J. 2005, *ApJ*, 630, 368
- Andersson, B.-G., Lazarian, A., & Vaillancourt, J. E. 2015, *ARA&A*, 53, 501
- Bernstein, M. P., Sandford, S. A., Allamandola, L. J., et al. 1999, *Science*, 283, 1135
- Bethell, T. J., Chepurnov, A., Lazarian, A., & Kim, J. 2007, *ApJ*, 663, 1055
- Caselli, P., & Ceccarelli, C. 2012, *The A&A Review*, 20, 151
- Chrysostomou, A., Hough, J. H., Whittet, D. C. B., et al. 1996, *ApJL*, 465, L61
- Collings, M. P., Anderson, M. A., Chen, R., et al. 2004, *MNRAS*, 354, 1133
- Cook, A. M., Ricca, A., Mattioda, A. L., et al. 2015, *ApJ*, 799, 14
- Cuppen, H. M., Walsh, C., Lamberts, T., et al. 2017, *Space Science Reviews*, 212, 1
- Cuytle, S. H., Allamandola, L. J., & Linnartz, H. 2014, *A&A*, 562, A22
- Draine, B. T. 2011, *Physics of the Interstellar and Intergalactic Medium* (Princeton, NJ: Princeton Univ. Press)
- Draine, B. T., & Lazarian, A. 1998, *ApJ*, 508, 157
- Draine, B. T., & Weingartner, J. C. 1996, *ApJ*, 470, 551
- Fayolle, E. C., Oberg, K. I., Garrod, R. T., van Dishoeck, E. F., & Bisschop, S. E. 2015, *A&A*, 576, A45
- Garrod, R. T. 2013, *ApJ*, 765, 60
- Greenberg, J. M., & Li, A. 1996, *A&A*, 309, 258
- Greenberg, J. M., & Li, A. 1997, *Advances in Space Research*, 19, 981
- Hasegawa, T. I., Herbst, E., & Leung, C. M. 1992, *Astrophysical Journal Supplement Series* (ISSN 0067-0049), 82, 167
- Herbst, E., & van Dishoeck, E. F. 2009, *ARA&A*, 47, 427
- Herranen, J., Lazarian, A., & Hoang, T. 2019, *ApJ*, 878, 0
- Hoang, T. 2019, *ApJ*, 876, 13
- Hoang, T., Cho, J., & Lazarian, A. 2018, *ApJ*, 852, 129
- Hoang, T., Draine, B. T., & Lazarian, A. 2010, *ApJ*, 715, 1462
- Hoang, T., & Lazarian, A. 2008, *MNRAS*, 388, 117
- Hoang, T., & Lazarian, A. 2009, *ApJ*, 695, 1457
- Hoang, T., Lazarian, A., & Andersson, B.-G. 2015, *MNRAS*, 448, 1178
- Hoang, T., & Tram, L. N. 2019, arXiv:1902.06438, submitted to *Nature Communications*
- Hoang, T., Tram, L. N., Lee, H., & Ahn, S.-H. 2019, *Nature Astronomy*, 3, 766
- Hollenbach, D. J., & Tielens, A. G. G. M. 1999, *Reviews of Modern Physics*, 71, 173

- Jones, A. P., Fanciullo, L., Köhler, M., et al. 2013, *A&A*, 558, 62
- Lazarian, A., Andersson, B.-G., & Hoang, T. 2015, in *Polarimetry of stars and planetary systems*, ed. L. Kolokolova, J. Hough, & A.-C. Levasseur-Regourd ((New York: Cambridge Univ. Press)), 81
- Lazarian, A., & Hoang, T. 2007a, *MNRAS*, 378, 910
- Lazarian, A., & Hoang, T. 2007b, *ApJ*, 669, L77
- Leger, A., Jura, M., & Omont, A. 1985, *A&A*, 144, 147
- Mathis, J. S., Mezger, P. G., & Panagia, N. 1983, *A&A*, 128, 212
- Michoulier, E., Noble, J. A., Simon, A., Mascetti, J., & Toubin, C. 2018, *Physical Chemistry Chemical Physics*, 20, 8753
- Mumma, M. J., Weissman, P. R., & Stern, S. A. 1993, In: *Protostars and planets III (A93-42937 17-90)*, 1177
- Oberg, K. I. 2016, *Chemical Reviews*, 116, 9631
- Oberg, K. I., Boamah, M. D., Fayolle, E. C., et al. 2013, *ApJ*, 771, 95
- Oberg, K. I., Bottinelli, S., Jørgensen, J. K., & van Dishoeck, E. F. 2010, *ApJ*, 716, 825
- Oberg, K. I., Fuchs, G. W., Awad, Z., et al. 2007, *ApJ*, 662, L23
- Öberg, K. I., Garrod, R. T., van Dishoeck, E. F., & Linnartz, H. 2009, *A&A*, 504, 891
- Oberg, K. I., Linnartz, H., Visser, R., & van Dishoeck, E. F. 2009, *ApJ*, 693, 1209
- Potapov, A., Theulé, P., Jäger, C., & Henning, T. 2019, *arXiv.org*
- Purcell, E. M. 1979, *ApJ*, 231, 404
- Spaans, M., Hogerheijde, M. R., Mundy, L. G., & van Dishoeck, E. F. 1995, *ApJ*, 455, L167
- Tielens, A. G. G. M., & Allamandola, L. J. 1987, in IN: *Physical processes in interstellar clouds; Proceedings of the NATO Advanced Study Institute, NASA, Ames Research Center, Moffett Field, CA; California, University, Berkeley*, 333–376
- Tielens, A G G M. 2007, *The Physics and Chemistry of Interstellar Medium (Cambridge University Press: San Diego, CA)*, 1–510
- Tram, L. N., & Hoang, T. 2019, *arXiv:1902.01921*, submitted to *ApJ*
- van Dishoeck, E. F. 2014, *Faraday Discussions*, 168, 9
- van Dishoeck, E. F. 2017, *arXiv:1710.05940*, 3
- van Dishoeck, E. F., Herbst, E., & Neufeld, D. A. 2013, *Chemical Reviews*, 113, 9043
- Watson, W. D., & Salpeter, E. E. 1972, *ApJ*, 174, 321
- Whittet, D. C. B., Bode, M. F., Longmore, A. J., Baines, D. W. T., & Evans, A. 1983, *Nature*, 303, 218
- Whittet, D. C. B., Hough, J. H., Lazarian, A., & Hoang, T. 2008, *ApJ*, 674, 304
- Work, A., & Lian, Y. 2018, *Progress in Aerospace Sciences*, 1